Cooperativity Mutants of Bacteriophage λ cI Repressor: Temperature Dependence of Self-Assembly†

David S. Burz‡ and Gary K. Ackers*

Department of Biochemistry and Molecular Biophysics, Washington University School of Medicine, St. Louis, Missouri 63110

Received August 30, 1995; Revised Manuscript Received December 11, 1995⊗

ABSTRACT: Analytical ultracentrifugation was used to study higher order self-assembly of λ cI repressors, including eight mutants whose monomer to dimer reactions were recently characterized [Burz *et al.* (1994) *Biochemistry 33*, 8399]. Six of the mutants were found to remain dimeric up to 50 μM total protein; the remaining mutants (EK102 and PT158) were found to undergo higher order oligomerization, as does wild-type cI. For these three repressors, we determined the stoichiometries and energetics of higher order assembly over the temperature range 5−40 °C. Weak dimerization exhibited by two other mutants, SN228 and SR228, was also evaluated by sedimentation equilibrium over this same temperature range. The end-state for higher order assembly of wild-type cI was determined to be octameric, in agreement with Senear *et al.* [(1993) *Biochemistry 32*, 6179−6189]. The assembly free energies resolved by the sedimentation analysis program NONLIN [Johnson, M. L., *et al.* (1981) *Biophys. J. 36*, 575−588] leads to the prediction that tetramers may contribute significantly to the intermediate populations during assembly. This analysis of the species populations is in accord with recent conclusions from fluorescence anisotropy studies [Banik *et al.* (1993) *J. Biol. Chem. 268*, 3938]. It was found that two of the mutant repressors (EK102 and PT158) assemble into octamers, but with differing possible intermediates. PT158 satisfies the stoichiometry $8M_1 \leftrightarrow 2M_4 \leftrightarrow M8$, while the EK102 data conforms to a $4M_2 \leftrightarrow 2M_4 \leftrightarrow M_8$ model, similar to WT (both the EK102 and WT data could also be described by a dimer−octamer model with no intermediates). Of the six repressors found in this study to remain dimeric, three exhibit non-cooperative DNA binding (GD147, KN192, YH210), two express intermediate cooperativity (EK188, SR228), and one is fully cooperative (SN228). The three octamerizing repressors are fully cooperative [Burz & Ackers (1994) *Biochemistry 33*, 8399], suggesting a correlation between their ability to form higher order assemblies and to engage in cooperative DNA binding. Linear van't Hoff plots were obtained for overall assembly of wild-type and EK102 dimers, while that of PT158 monomers was curved, indicating a negative heat capacity change. The van't Hoff analyses of dimerization constants for SN228 and SR228 were distinctly different from each other and also from that of wild type; such differences might be related to the disparate cooperative behavior found previously for these mutants (Burz & Ackers, 1994).

Regulation of biological function involves interactions between macromolecules, that are in turn controlled by temperature and by interactions with small molecules, protons, and specific ions (Ca^{2+}, Mg^{2+}). In order to construct predictive, *in vivo* models of macromolecular regulation, it is necessary to understand the linkages between interactions observed *in vitro*, and how they respond to changing thermodynamic variables. This understanding is especially critical when the process of interest involves a self-associating macromolecular ensemble. Such is the case with the bacteriophage λ cI repressor where dimerization of repressor monomers occurs in the nanomolar range for wild-type protein (Beckett *et al*., 1991) and wild-type dimers associate to tetramers and octamers at micromolar concentrations (Banik *et al*., 1993; Senear *et al*., 1993). Thermodynamic linkages between the formation of dimers and their cooperative DNA binding provide multiple avenues of control over occupancy of the operator sites that regulate transcription of the *cro* and cI repressor genes, and hence the switch between lysogenic and lytic growth [for a review, see Ptashne (1992), Johnson, A. D., *et al*. (1981), Ackers *et al*. (1982), Shea and Ackers (1985), and Burz and Ackers (1994)]. A wealth of information exists regarding the energetics of repressor dimer interactions with λ right operator DNA (O_R) [see Brenowitz *et al*. (1986)], and the linkage of those processes to pH (Senear & Ackers, 1990), salt (Koblan & Ackers, 1991b; Senear & Batey, 1991), and temperature (Koblan & Ackers, 1992; Merabet & Ackers, 1995). However, as yet no specific function has been convincingly ascribed to the higher order oligomers.

The mutant repressors used in this study, except for PT158, were isolated using genetic functional screens designed to select for deficiencies in pairwise cooperative DNA binding (Beckett *et al*., 1993; Benson *et al*., 1994). PT158 was isolated as an *ind*$^+$ mutation, displaying increased susceptibility to *recA*-mediated cleavage (Gimble & Sauer, 1989). Additionally, all repressors used in these studies contain a single amino acid replacement in the C-terminal domain, except EK102, whose mutation is located in the linker region (aa 93−133) between the N-terminal and C-terminal do-

† This work was supported by NIH Grants GM39343 and R37-GM24486 (G.K.A.).

* Author to whom correspondence should be addressed.

‡ Present address: Wadsworth Center, New York State Department of Health, Axelrod Institute, Albany, NY 12202-2002.

⊗ Abstract published in *Advance ACS Abstracts,* February 1, 1996.

0006-2960/96/0435-3341$12.00/0

mains. The C-terminal domain mediates the cooperative and self-association properties exhibited by cI repressor (Brack & Pirotta, 1975; Pabo *et al*., 1979; Beckett *et al*., 1993, Benson *et al*., 1994; Burz *et al*., 1994; Burz & Ackers, 1994; Bandyopadhyay *et al*., 1995), while the N-terminal domain mediates protein−DNA contacts.

In previous studies (Burz *et al*., 1994; Burz & Ackers, 1994), we found a wide range of dimerization and DNA binding properties for these mutants. Dimerization equilibria were characterized as a prelude to quantitative footprint studies of mutant repressor binding to right operator DNA. That study, ranging from $\sim 10^{-12}$ to 10^{-6} M in total protein concentration, revealed two repressors that dimerize 2−3 kcal/mol more weakly than wild type (SN228 and SR228); one that oligomerizes with no detectable dimeric intermediate (PT158), and four that dimerize with wild-type energetics (EK102, GD147, KN192, and YH210).

In this work, we extend the self-assembly analyses for wild-type and mutant cI repressors from ~1 to 50 μM, using sedimentation equilibrium. These experiments provide estimates of the stoichiometries and free energies of self-association. We show that six repressors do not assemble beyond dimers (GD147, EK188, KN192, YH210, SN228, and SR228); two of the dimerizing repressors also form octamers (WT and EK102) while one repressor (PT158) assembles to octamers without dimeric intermediates. Our results are consistent with earlier evidence supporting a significant population of tetramers along the assembly pathway for the oligomerizing repressors (Banik *et al.*, 1993). In addition, the temperature dependencies of these assembly reactions were determined over the range 5−40 °C, and the changes in enthalpy and heat capacity accompanying these processes were estimated.

The combination of accurate footprint titration data and preliminary estimates of the propensity of certain mutant repressors to form assembly states greater than dimer suggested a possible correlation between oligomerization and cooperative binding to operator DNA (Burz & Ackers, 1994). Specifically, five of the six repressors that form dimers as the limiting species in self-assembly are defective in cooperativity (the exception being SN228, which is fully cooperative), and no mutant that oligomerizes beyond dimers shows any loss of cooperative binding (i.e., EK102 and PT158). These observations raise a number of questions that bear on the regulatory implications of cI repressor octamers and, therefore, the life cycle of the bacteriophage. What are the oligomeric states and self-association energetics of these repressors? Are there mechanistic relationships between higher order oligomerization and cooperativity? Does oligomerization exhibit the same thermodynamic signature as other processes in which the cI repressor participates? Are there functional processes that can be attributed specifically to the formation of oligomers?

MATERIALS AND METHODS

Chemicals and Biochemical Materials. Ampicillin, bovine serum albumin (BSA), isopropyl-β-D-thiogalactoside (IPTG), lysozyme, phenylmethanesulfonyl fluoride (PMSF), polyethylene immine (PEI), and Sephadexes were from Sigma Chemical Co. Electrophoresis-grade acrylamide, ammonium persulfate, bis(acrylamide), and TEMED were obtained from Bio-Rad. Acrylamide and bis(acrylamide) were deionized using Bio-Rad AG501-X8 mixed-bed resin prior to use. Affi-Gel Blue affinity resin was from Bio-Rad. Hydroxyapatite-Ultrogel (HAP-Ultrogel) was from IBF Biotechnics. All other chemicals were reagent or analytical grade.

Protein Purification. Repressors were overexpressed from the *tac* promoter on plasmid pEA300 (Amman *et al*., 1983) for wild type or pFG600 (Gimble and Sauer, 1989) for the mutants (Beckett *et al*., 1993) and purified from *Escherichia coli* strain X90 as described (Johnson, 1980; Beckett *et al.*, 1993). The purification properties and yields of the mutant repressors were similar to those of wild type. All preparations were deemed >95% pure by Coomassie Brilliant Blue staining of samples electrophoresed on 8% SDS polyacrylamide gels (Laemmli, 1970). Total monomer concentration of the unlabeled repressor was measured by UV absorbance at 280 nm, assuming an extinction coefficient of 1.18 mL mg^{-1} cm^{-1} (Sauer & Anderegg, 1978).

Sedimentation Equilibrium. Experiments were performed using a Beckman XL-A Ultima analytical ultracentrifuge equipped with a Ti-60a 4-hole titanium rotor, 6- or 2-channel 12 mm thick charcoal-filled epon centerpieces, and quartz windows. Absorbance optics were used to monitor the optical density at 280 nm for all experiments; the range of data was truncated to exclude values above 1.6 OD. Repressor samples were prepared either by dialysis or by dilution of repressor stock solutions into standard buffer, SB (10 mM Bis-Tris, pH 7.0, at 20 °C, 200 mM KCl, 2.5 mM $MgCl_2$, and 1.0 mM $CaCl_2$). Sample volumes were 100 μL of repressor plus 20 μL of FC43 (fluorocarbon-43; Beckman) for channels A and B in the 6-channel cells and 90 μL of repressor plus 30 μL of FC43 in channel C. FC43 is an inert oil that displaces the sample away from the bottom of the cells, improving data acquisition. Control experiments demonstrated that the oil did not affect the resolved energetics (not shown). Loading concentrations ranged from 0.1 to 3.0 mg/mL at a concentration ratio of ~1:3:10; however, useful data were generally not obtained at loading concentrations greater than ~1.2 mg/mL in channel A. Experimental speeds ranged from 10 000 to 45 000 rpm. Data were collected as an average of four scans at radial increments of 0.001 cm from 5.9 to 7.2 cm.

Reduced molecular weights, σ, were calculated from repressor concentration distributions at equilbrium according to

$$\partial \ln c_{r,i} / \partial(r^2/2) = \sigma_i \quad (1)$$

where

$$\sigma_i = M_i(1 - \bar{V}\rho)\omega^2/RT \quad (2)$$

$c_{r,i}$ is the concentration of repressor species i at radial position r, M_i is the anhydrous molecular weight of the ith species, $\bar{V}$ is the partial specific volume of anhydrous macromolecule, ρ is solvent density, ω is rotor speed, R is the gas constant in erg cm^{-1} K^{-1} and T is absolute temperature. Solvent density was calculated using tabulated values (Laue *et al*., 1992) and ranged from $\rho = 1.009$ at 5 °C to $\rho = 1.001$ at 40 °C. Values were calculated from the mass composition average of partial specific volumes for each amino acid and corrected for temperature using the empirical formulas given in Laue *et al*. (1992); a value of 0.735 mL/g was used for wild-type repressor at 20 °C. Variation of these parameters

with pH was not considered; the pH was 7.00 ± 0.17 over the range examined.

Raw data were truncated to the appropriate range of optical density, (nominally 0.10−1.6 OD_{280}) using REEDIT, and simultaneous analyses of 6−12 channels of data were carried out to resolve stoichiometry and assembly equilibrium constants using the nonlinear least squares program NONLIN (Johnson, M. L., *et al.*, 1981); executable versions of both programs were kindly provided by Dr. David Yphantis (University of Connecticut, Storrs, CT). The lowest optical densities acquired from any data set were easily defined for the meniscus, but the steepness of the concentration gradient at the base of the cell was found to produce small "steps" in the resolved optical trace of the data due to the changing index of refraction accompanying the gradient. The high absorbance data were successively truncated to yield a single species fit of the data set with a standard deviation of 0.004−0.10. Models employing various assembly stoichiometries were examined in accordance with the following equations:

$$Y_r = \delta_j + \sum_{i=1}^{m} \exp(\gamma_i) \tag{3}$$

$$\gamma(1) = \ln A_i + \sigma(r^2/2 - r_o{}^2/2) \tag{4}$$

$$\gamma(>1) = N\gamma(1) + \ln K_N \tag{5}$$

where Y_r is the absorbance at radius r, δ_j is the baseline offset for the jth experiment, A_i is the monomer absorbance at reference radius r_o, K_N is the association constant for the reaction: $NM \leftrightarrow M_N$. Assembly free energies were calculated using the relationship $\Delta G_N = -RT \ln K_N$. Nonideality was not included.

Determination of Assembly Free Energies. Resolution of equilibrium constants by the analysis program NONLIN (Johnson, M. L., *et al.*, 1981) assumes that self-association occurs from a single molecular weight species. For example, expanding eq 3 to consider three species for an assembly model involving dimers in association equilibria with tetramers and with octamers, the following expressions are obtained:

$$Y_r = \delta_j + \exp[\ln A_j + \sigma(r^2/2 - r_o{}^2/2)] + \exp\{2[\ln A_j + \sigma(r^2/2 - r_o{}^2/2)] + \ln K_2\} + \exp\{4[\ln A_j + \sigma(r^2/2 - r_o{}^2/2)] + \ln K_4\} \tag{6}$$

$$Y_r = \delta_j + A_{j_o} \exp[\sigma(r^2/2 - r_o{}^2/2)] + K_2(A_{j_o} \exp[\sigma(r^2/2 - r_o{}^2/2)])^2 + K_4(A_{j_o} \exp[\sigma(r^2/2 - r_o{}^2/2)])^4 \tag{7}$$

By substituting $[A_{o,r}]$ for $A_{j_o}\exp[\sigma(r^2/2 - r_o{}^2/2)]$, the monomer absorbance distribution from the meniscus (reference) to radial position r, we can write

$$Y_r = \delta_j + [A_{o,r}] + K_2[A_{o,r}]^2 + K_4[A_{o,r}]^4 \tag{8}$$

which provides the experimental distribution of mass in the cell, *i.e.*, the distribution of self-associated species over the concentration range present from the experimental meniscus to the bottom of the cell. More importantly, it implies self-association reactions of the following types:

$$2M_2 \overset{K_2}{\leftrightarrow} M_4 \qquad 4M_2 \overset{K_4}{\leftrightarrow} M_8 \tag{9}$$

i.e., each association complex (M_4 or M_8) is characterized by its equilibrium constant for overall assembly from "monomeric units" (e.g., dimers of eq 9).

By contrast the assembly of dimers to octamers with a tetrameric intermediate is conventionally written using stepwise equilibrium constants:

$$2M_2 \overset{k_{24}}{\leftrightarrow} M_4 \qquad 2M_4 \overset{k_{48}}{\leftrightarrow} M_8 \tag{10}$$

where K_2 of eq 9 is equivalent to k_{24} of eq 10. By conservation of energy, we have

$$K_4 = (k_{24})^2 \cdot k_{48} \tag{11}$$

and

$$k_{48} = K_4/(k_{24})^2 \tag{12}$$

Each experimental equilibrium constant (e.g., K_4) is based on the macromolecular species absorbance (mass) distribution throughout the sector and is converted from absorbance (mass) to molar units by the expression (Yphantis, 1964):

$$K_M = K_{abs}([M_o]^{n-1}/n)(\epsilon b)^{n-1} \tag{13}$$

where ϵ is the extinction coefficient in mL mg^{-1} cm^{-1}, b is the cell path length (1.2 cm), n is the assembly stoichiometry, K_{abs} is the absorbance equilibrium constant resolved by the analysis, K_M is the molar equilibrium constant, and M_o is molecular weight of the assembling or "monomeric" species. The monomer molecular weight of wild-type cI repressor was 26 081 ± 3 as determined by electrospray mass spectroscopy and corroborated by the mass-average amino acid composition-derived molecular weight. We used molecular masses of 26 100 and 52 200 Da for all calculations involving wild-type and mutant monomers and dimers, respectively. The extinction coefficient was found to vary by 1% at 40 and 5 °C relative to 20 °C; this was deemed insignificant with respect to values of the resolved equilibrium constants assuming constancy of ϵ and was not considered in the calculation of equilibrium constants.

Calculation of Species Populations. Calculations of species population distributions from the resolved assembly free energies were carried out by formulating a partition function (Z) that describes concentration dependence of repressor oligomerization. For example, the total protein concentration for a monomer−dimer−tetramer−octamer assembly model is

$$C_{TOT} = [M_1] + 2[M_2] + 4[M_4] + 8[M_8] \tag{14}$$

where concentrations $[M_i]$ are in units of species molarity. Using stepwise equilibrium constants (eq 10) and substituting $[X] = [M_1]$, we can write the following partition function in monomer concentration units:

$$Z = [X] + 2k_{12}[X]^2 + 4k_{12}^2k_{24}[X]^4 + 8k_{12}^4k_{24}^2k_{48}[X]^8 \tag{15}$$

Table 1: Molecular Weights for Dimeric Mutant cI Repressors

protein	temp (°C)	σ_{calcd}[a]	σ_{msrd}	MW	SD[b]
GD147	20	0.611	0.599 [0.595−0.603]	51200 ± 350	0.0057
GD147	40	0.564	0.562 [0.555−0.569]	52000 ± 650	0.0054
EK188	20	0.606	0.630 [0.621−0.639]	54200 ± 800	0.0069
EK188	40	0.559	0.559 [0.552−0.567]	52100 ± 700	0.0067
KN192	20	0.611	0.589 [0.583−0.595]	50300 ± 500	0.0085
KN192	40	0.564	0.540 [0.532−0.548]	50000 ± 750	0.0067
YH210	20	0.611	0.593 [0.583−0.602]	50600 ± 800	0.0081
YH210	40	0.564	0.525 [0.515−0.536]	48600 ± 950	0.0098

[a] Reduced molecular weight calculated using eq 2 and assuming a value of 52200 for repressor dimers. [b] Standard deviation in optical density units.

Defining the mass fraction f_i of each species:

$$f_i = [M_j]/Z \tag{16}$$

we then have, for monomers, dimers, tetramers, and octamers:

$$f_1 = [X]/Z \tag{17a}$$

$$f_2 = 2k_{12}[X]^2/Z \tag{17b}$$

$$f_4 = 4k_{12}^2k_{24}[X]^4/Z \tag{17c}$$

$$f_8 = 8k_{12}^4k_{24}^2\,k_{48}[X]^8/Z \tag{17d}$$

representing the fraction of total mass present as monomers, dimers, tetramers, and octamers, respectively. The molar concentration of each species in monomer units is given by

$$[X_i] = f_i\,(C_{TOT}) \tag{18}$$

where C_{TOT} is total protein expressed in monomer concentration units. Dividing $f_i\,(C_{TOT})$ by the stoichiometry (i) will yield the concentration in molar units of X_i.

RESULTS

Sedimentation Equilibrium Experiments. We find that mutation of the C-terminal residues most commonly compromises oligomerization by eliminating assembly beyond dimers. Six of the nine repressors studied did not assemble beyond dimers at either 20 or 40 °C. Data for GD147, EK188, KN192, and YH210 were best fit assuming a nonassociating species. Molecular weights estimated from global analysis of all data for each of the four mutant repressors that dimerize with wild type energetics (∼−11 kcal/mol) are summarized in Table 1. Our measured molecular weights are in good agreement with the value calculated for a dimer (52160). Weakened dimerization at 40 °C may be responsible for the slight reduction in molecular weight resolved for KN192 and YH210. The molecular weight for EK188 at 20 °C was consistently resolved at a slightly larger value than expected. However no further assembly was observed, even at loading concentrations up to 3 mg/mL (∼115 μM).

Apparent molecular weights resolved from a global fit of the SN228 data and SR228 data were lower than dimeric at all temperatures examined, reflecting the mixed populations of monomers and dimers (∼67% SN228 dimers, ∼85% SR228 dimers; not shown). It was found previously that these repressors exhibit weak dimerization (Burz *et al.*, 1994). Their equilibrium constants are discussed below.

Table 2: Assembly Energetics for Higher Order Assembly of Wild Type and EK102 cI Dimers

	$[4M_2 \leftrightarrow M_8]$		$[4M_2 \leftrightarrow 2M_4 \leftrightarrow M_8]$		
temp (°C)	ΔG_{28}[a]	SD[b]	ΔG_{24}	ΔG_{48}	SD
			Wild Type		
5	−21.9 ± 0.3	0.0061	−7.21 ± 0.23	−8.4 ± 0.7	0.0060
10	−21.6 ± 0.3	0.0079	−7.27 ± 0.23	−8.1 ± 0.7	0.0074
15	−21.9 ± 0.2	0.0074	−7.90 ± 0.22	−7.7 ± 0.7	0.0058
20	−22.3 ± 0.2	0.0067	−7.22 ± 0.21	−8.7 ± 0.6	0.0063
25	−22.4 ± 0.2	0.0087	−7.31 ± 0.23	−8.5 ± 0.7	0.0083
30	−22.2 ± 0.2	0.0075	−7.48 ± 0.18	−8.1 ± 0.6	0.0063
35	−22.5 ± 0.1	0.0054	−7.26 ± 0.15	−8.7 ± 0.5	0.0047
40	−22.7 ± 0.1	0.0063	−6.93 ± 0.23	−9.2 ± 0.6	0.0060
			EK102		
5	−21.7 ± 0.3	0.0078	−8.26 ± 0.32	−7.0 ± 0.5	0.0067
10	−22.0 ± 0.2	0.0059	−6.83 ± 0.21	−8.9 ± 0.2	0.0058
15	−22.0 ± 0.2	0.0049	−6.78 ± 0.19	−8.9 ± 0.2	0.0048
20	−22.2 ± 0.2	0.0081	−7.85 ± 0.23	−7.9 ± 0.3	0.0070
25	−22.1 ± 0.2	0.0078	−6.78 ± 0.22	−9.0 ± 0.2	0.0076
30	−22.1 ± 0.2	0.0087	−7.58 ± 0.19	−8.0 ± 0.2	0.0074
35	−22.5 ± 0.2	0.0065	−7.42 ± 0.16	−8.3 ± 0.2	0.0055
40	−22.4 ± 0.1	0.0070	−6.56 ± 0.19	−9.6 ± 0.1	0.0068

[a] Subscripts denote the stoichiometry of the assembly reaction. Equilibrium constants are related to the free energy by the conventional relationship, $\Delta G = -RT \ln K$. ΔG_{48} is calculated from the following expression: $\Delta G_4 = 2\Delta G_2 + \Delta G_{48}$ where ΔG_2 and ΔG_4 are the free energies corresponding to K_2 and K_4, the equilibrium constants resolved by the fitting program (see text, eq 9). [b] Standard deviation in OD units.

Table 3: Assembly Energetics for PT158 cI Monomers

	$[8M \leftrightarrow M_8]$		$[8M \leftrightarrow 2M_4 \leftrightarrow M_8]$		
temp °C	ΔG_{18}[a]	SD[b]	ΔG_{14}	ΔG_{48}	SD
5	−48.5 ± 0.4	0.0060	−20.9 ± 0.3	−8.0 ± 1.0	0.0050
10	−49.3 ± 0.4	0.0076	−20.3 ± 0.4	−9.4 ± 1.2	0.0074
15	−49.7 ± 0.4	0.0071	−20.2 ± 0.3	−9.7 ± 0.9	0.0070
20	−50.6 ± 0.4	0.0060	−21.3 ± 0.3	−9.1 ± 0.9	0.0054
25	−51.7 ± 0.4	0.0062	−22.0 ± 0.4	−8.7 ± 1.0	0.0050
30	−51.9 ± 0.5	0.0097	−22.1 ± 0.4	−8.9 ± 0.3	0.0090
35	−52.1 ± 0.4	0.0059	−21.8 ± 0.3	−9.0 ± 1.0	0.0052
40	−50.2 ± 0.3	0.0076	−21.1 ± 0.2	−9.0 ± 0.7	0.0060

[a] Subscripts denote the stoichiometry of the assembly transition. Equilibrium constants are related to the free energy by the conventional relationship, $\Delta G = -RT \ln K$. ΔG_{48} is calculated from the following expression: $\Delta G_8 = 2\Delta G_4 + \Delta G_{48}$ where ΔG_4 and ΔG_8 are the free energies corresponding to K_4 and K_8, the equilibrium constants resolved by the fitting program (see text). [b] Standard deviation in OD units.

Apparent molecular weights resolved from global fitting to a single molecular species model for wild type, EK102, and PT158 demonstrated self-assembly beyond dimers; typical data are shown in Figure 1 for EK102. The effect of increasing molecular weight at higher protein concentrations on the macromolecular distribution is evident from the sharp increase in optical density at the bottom of the cell coupled with a pronounced reduction in the meniscus OD as rotor speed is raised. The higher molecular weight species migrate further in the centrifugal field, increasing in concentration at the expense of dimers. As temperature increases, a decrease in weight average mass is observed, consistent with a reduced state of assembly.

Self-Assembly Model Parameters. Since the monomeric molecular weight is accurately known, holding this term fixed in the fitting process is justified. However, in order to

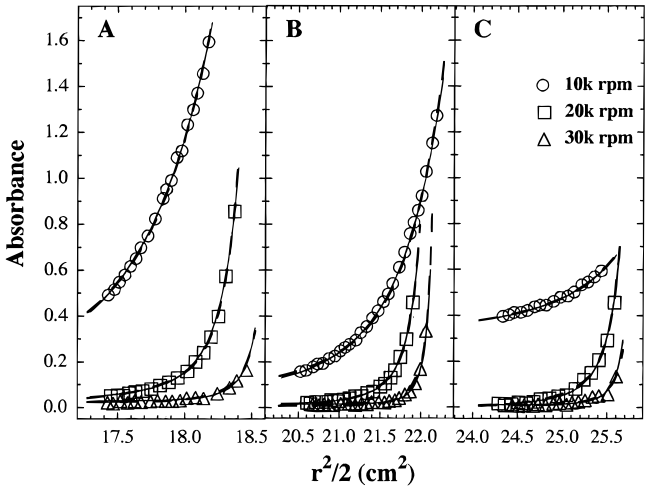

FIGURE 1: Sedimentation equilibrium data for EK102 at 30 °C. Loading concentrations, in total monomer, are (A) 1.1, (B) 0.34, and (C) 0.12 mg/mL. Fits shown are for dimer−tetramer−octamer (—) and dimer−octamer (− −) assembly models. For clarity, only every fifth, sixth, or seventh data point is shown.

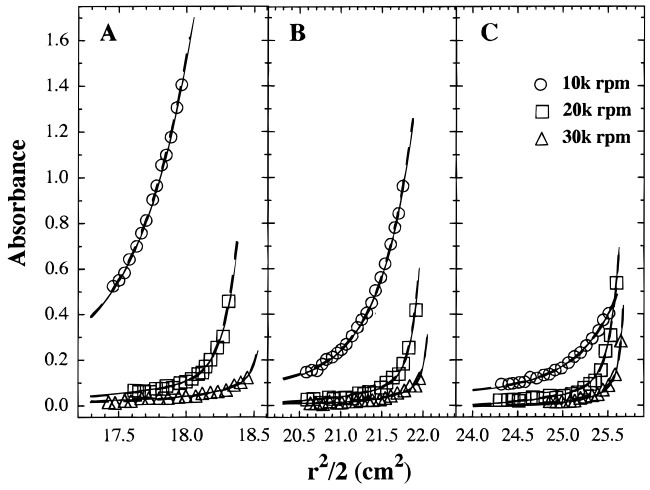

FIGURE 2: Sedimentation equilibrium data for PT158 at 15 °C. Loading concentrations, in total monomer, are (A) 1.1, (B) 0.35, and (C) 0.12 mg/mL. Fits shown are for monomer−tetramer−octamer (—) and monomer−octamer (− −) assembly models. For clarity, only every fifth, sixth, or seventh data point is shown.

evaluate internal consistency of the data, combinations of *M* and *N* were held fixed during least squares minimization. When molecular weight was treated as a fitted parameter, values consistent with assembly of dimers were obtained for wild type and EK102. For PT158 and SN228, values consistent with monomer assembly were obtained. These observations are in accord with the properties determined by analytical gel chromatography using radiolabeled repressors (Burz *et al.*, 1994). SN228 and SR228 showed no systematic deviation in fitted molecular weights, virtually all values were within ±2% of the atomic weight units of monomer.

N was floated at fixed molecular weight to test the validity of stoichiometries used in the final analyses. For assembly of wild-type and EK102 dimers, the overall resolved stoichiometry was 3.5−4.0, using either the dimer−octamer or the dimer−tetramer−octamer models, consistent with the integral stoichiometries used in the initial analyses. For PT158, the stoichiometry of assembly of monomeric units was found to be 7.1−7.9; attempts to fit the data to models involving assembly from dimers or from monomers to alternative stoichiometries resulted in highly skewed residuals (not shown). For the weakly dimerizing proteins, SN228 and SR228, the stoichiometry was always found to be 2.0 ± 0.1. In general, the agreement between fixed and fitted molecular weights, stoichiometries, and corresponding free energies of assembly was quite good. With this observation in hand, all subsequent data fits on oligomerizing repressors were performed using a fixed molecular weight and an end-state stoichiometry of four dimeric or eight monomeric units.

Wild Type and EK102 Form Octamers. Wild-type repressor assembly data was similar to that reported by Senear *et al*. (1993). Likewise, EK102 repressor data was similar to that obtained for wild type at all temperatures examined. Our data were equally well-described by either a transition of dimers to octamers (with no intermediates) or by a dimer−tetramer−octamer stoichiometry (Figure 1); free energies are presented in Table 2. Standard errors of the fits to the model invoking the tetrameric intermediate were consistently smaller. However, a more revealing criterion for assessing the best fit to a given model of assembly consists of examining the residuals. Systematic deviations were observed in the global residuals (not shown) for all but the dimer−octamer and dimer−tetramer−octamer models. Correspondingly, the trace of the fitted curve through the data shows systematic deviations when analyzed using models other than those shown in Table 2. The free energy resolved for the assembly of wild-type dimers to octamers at 20 °C was −22.3 ± 0.2 kcal/mol of octamer formed, in reasonable agreement with −22.9 ± 0.2 kcal/mol of octamer reported by Senear *et al*. (1993). Similar results were obtained using a dimer−tetramer−octamer assembly model: We resolved −7.2 ± 0.2 kcal/mol of tetramer and −23.1 ± 0.2 kcal/mol of octamer formed from dimers, while Senear *et al*. (1993) found −7.0 ± 0.1 kcal/mol of tetramer and −23.0 ± 0.1 kcal/mol of octamer, respectively. Our EK102 data yielded comparable free energies for these two reaction models that were essentially identical with those of WT repressor (Table 2).

PT158 Self-Assembles from Monomers. The lowest apparent molecular weight resolved from a single channel analysis of PT158 is consistent with assembly from a molecular weight species smaller than dimer (not shown). The data for PT158 are best described by either of the two models: a transition of monomers to octamers with no intermediates or a monomer−tetramer−octamer assembly. These results were in accord with our analytical gel chromatography data showing PT158 to be monomeric at concentrations below ∼1 μM, thereupon associating to a species larger than dimer (Burz *et al*., 1994). Sedimentation results for PT158 are shown in Figure 2; the sharp increase in OD at the base of the cell is similar to that observed for wild type and EK102; however, a major distinction lies in panel C, the lowest loading concentration. Data at 10 000 rpm provided evidence of highly concerted assembly for this mutant relative to that of wild-type or EK102 repressors (see Figure 1), as indicated by a lower intrinsic absorbance associated with monomeric species at the meniscus. This data, when analyzed by a monomer to octamer model at 20 °C, yielded an assembly free energy of −50.6 ± 0.4 kcal/mol of octamer formed. By contrast, the stepwise free energies resolved for a monomer−tetramer−octamer assembly scheme were −20.1 ± 0.3 kcal/mol of tetramer

Table 4: Dimerization Free Energies for SN228 and SR228 cI Monomers

	SN228		SR228	
temp °C	ΔG_{12} (kcal/mol)	SD[a]	ΔG_{12} (kcal/mol)	SD
5	-6.02 ± 0.10	0.0057	-7.71 ± 0.19	0.0050
15	-6.83 ± 0.14	0.0047	-8.56 ± 0.26	0.0047
20	-7.06 ± 0.14	0.0062	-8.16 ± 0.22	0.0057
25	-6.81 ± 0.11	0.0054	-9.33 ± 0.32	0.0047
30	-7.12 ± 0.11	0.0077	-8.96 ± 0.27	0.0046
35	-7.29 ± 0.11	0.0053	-8.46 ± 0.22	0.0053
40	-7.41 ± 0.15	0.0051	-7.48 ± 0.15	0.0067

[a] Standard deviation of the global fit in OD units.

formed and -9.1 ± 0.9 kcal/mol of octamer formed from tetramers (Table 3). All three octamerizing repressors were found to have a similar free energy for the tetramer to octamer stage of assembly, suggesting a common mechanism not perturbed by the mutations EK102 or PT158.

Weakly Dimerizing Repressors. The weakened dimerization seen with SN228 and SR228, relative to wild type, shifts this equilbrium into a concentration range that is experimentally accessible under conditions of this study. At 20 °C, the dimerization free energies resolved for SN228 and SR228 were -7.1 ± 0.1 kcal and -8.2 ± 0.2 kcal, respectively (Table 4). These are in reasonable agreement with values obtained using analytical gel chromatography [-7.5 ± 0.2 kcal for SN228 and -8.8 ± 0.3 for SR228 (Burz *et al.*, 1994)]. In the case of mutant repressors that exhibit wild-type dimerization energetics, the free energy for the process is too negative to permit resolution of an equilibrium dimerization constant at 20 °C.

Temperature Dependence of Dimer Assembly. Equilibrium constants for assembly of wild-type and EK102 repressors were estimated between 5 and 40 °C using dimer−octamer and dimer−tetramer−octamer stoichiometries. The resolved assembly free energies were similar for both proteins and increased slightly with temperature for the dimer−octamer model; stepwise free energies for dimer−tetramer−octamer assembly showed no systematic variation with temperature (Table 2). A van't Hoff transformation of data for both repressors [$\partial \ln K/\partial(1/T) = -\Delta H/R$] is shown in Figure 3. The linear increase found in $\ln K_{28}$ with temperature yielded a van't Hoff enthalpy for assembly. Such a linear van't Hoff relationship indicates that both the enthalpy and heat capacity changes accompanying assembly are approximately constant over the temperature range examined [cf. Merabet and Ackers (1995)]. Data for the stepwise assembly constants suggest a slight positive slope for the dimer−tetramer reaction, whereas tetramer−octamer assembly data are essentially flat, suggestive of a very small enthalpy change. The van't Hoff enthalpies and their derivative ΔC_p values are summarized in Table 5.

Monomer Assembly. Free energies for assembly of PT158 monomers to octamers were found to decrease steadily with temperature by ~3 kcal from 5 to 35 °C and then to increase sharply by ~2 kcal over the range 35 and 40 °C (Table 3). Stepwise assembly free energies are found largely invariant with temperature. A van't Hoff plot of these data shows sharp curvature for the monomer to octamer model, indicating a strong thermal dependence of overall assembly enthalpy and a large heat capacity change associated with octamerization of these mutant repressor monomers (Figure 4). The van't Hoff enthalpies deduced from high and low temperature limbs of Figure 4 and the estimated values of ΔC_p are presented in Table 5. When PT158 assembly is analyzed using a monomer−tetramer−octamer model, the van't Hoff plot for the monomer−tetramer stage shows a slight positive slope, while that of the tetramer−octamer transition is relatively flat (Figure 4).

Dimerization equilibrium constants for SN228 and SR228 as a function of temperature are presented in Table 4. These results are in general agreement with their weakened dimer-

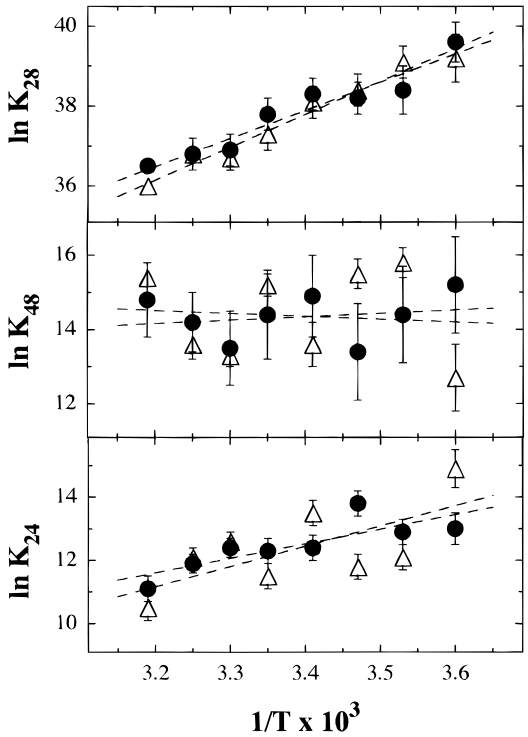

FIGURE 3: van't Hoff plots for wild-type and EK102 repressor self-assembly equilibrium constants. Subscripts denote stoichiometry of the stepwise process. Closed syumbols are wild-type data; open symbols represent EK102. Dotted lines represent best linear descriptions of the data from which apparent enthalpies were obtained.

Table 5: van't Hoff Enthalpies and Apparent Heat Capacity Changes for cI Assembly Processes

reaction	protein	ΔH_{vH}[a]	ΔC_p[b]	T_H (K)	T_S (K)
$[4M_2 \leftrightarrow M_8]$	WT	-14.0 ± 2.8	−0.1	205	349
	EK102	-16.3 ± 1.2	−0.2	214	320
$[2M_2 \leftrightarrow M_4]$	WT	-9.2 ± 4.3	−0.8	283	292
	EK102	-12.7 ± 9.3	−0.2	230	266
$[4M \leftrightarrow M_4]$	PT158	-10.2 ± 8.5	−0.8	283	308
$[2M_4 \leftrightarrow M_8]$	WT	-1.8 ± 6.0	0.9	297	288
	EK102	-1.6 ± 10.3	−0.2	294	337
	PT158	-6.8 ± 7.3	−1.2	290	297
$[8M \leftrightarrow M_8]$	PT158	-101 ± 37[c]	−3.2	287	302
	PT158	-7.8 ± 6[d]	−	−	−
$[2M \leftrightarrow M_2]$	SN228	3.6 ± 2.7	−0.5	302	316
	SR228	-47.1 ± 5.7[c]	−2.2	292	296
	SR228	8.4 ± 12[d]	−	−	−
	WT[e]	-15.1 ± 0.4	~0	280−310	~295

[a] Calculated from the slope of the van't Hoff plot, in kcal/mol; errors represent the 67% confidence interval. [b] Values for ΔC_p (kcal/mol·K), T_H (K), and T_S (K) were estimated as described in the text using the following equation: $\ln K_{ij} = (\Delta C_p/R)[T_H/T - \log(T_S/T) - 1]$. [c] High-temperature limb of van't Hoff plot. [d] Low-temperature limb of van't Hoff plot. [e] From Koblan and Ackers (1991a).

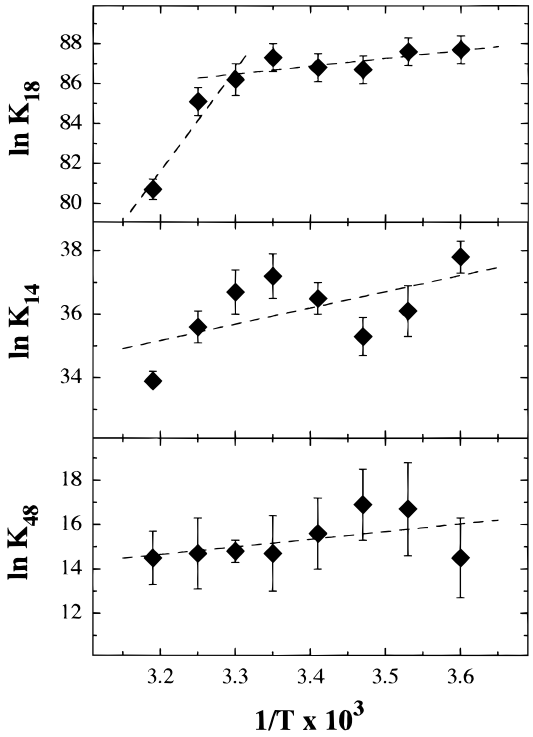

FIGURE 4: van't Hoff plots for PT158 repressor self-assembly equilibrium constants. Subscripts denote stoichiometry of the stepwise process. Dotted lines represent best linear descriptions of the data from which apparent enthalpies for the low and high temperature limbs were obtained.

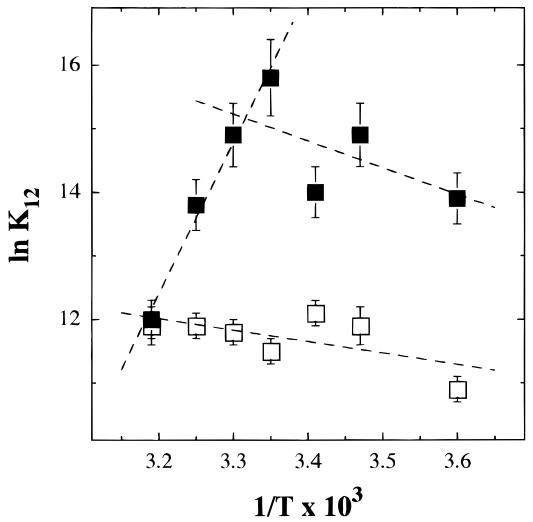

FIGURE 5: van't Hoff plot for SN228 and SR228 dimerization. Dotted lines represent best linear descriptions of the data from which apparent enthalpies for the low and high temperature limbs were obtained.

ization measured previously from analytical gel chromatography data (Burz *et al*., 1994). The free energy of dimerization for SN228 increases slightly with temperature, while that of SR228 exhibits a minimum at 25 °C increasing by ~2 kcal at 5 and 40 °C. A van't Hoff transformation of the resolved equilibrium constants is shown in Figure 5. The SN228 data are easily fit to a straight line, yielding an enthalpy of dimerization of +4.6 kcal/mol. Data for SR228 exhibits pronounced curvature suggesting an assembly mechanism that differs from that of wild type and SN228; the van't Hoff enthalpies estimated for the high and low temperature limbs of this plot are presented in Table 5.

Table 6: Self-Assembly and DNA Binding Properties of Wild Type and Mutant cI Repressors[a]

	self-association			DNA binding			
protein	dim	tet	oct	int	coop	NS	form
wild type	+	+	+	+	+	(+)	octamers
EK102	+	+	+	+	+	(+)	
PT158	0	+	+	+	+	(+)	
SN228	−	0	0	+	+	(0)	"weak" dimers
SR228	−	0	0	+	−	(0)	
GD147	+	0	0	+	0	(0)	"full" dimers
EK188	*	0	0	+	−	(+)	
KN192	+	0	0	+	0	(0)	
YH210	+	0	0	+	0	(0)	

[a] Symbols: (+) indicates wild-type free energy for the process; (−) indicates a weaker free energy (deficiency); (0) indicates apparent elimination of the process; (*) EK188 is dimeric, ΔG_{dim} was not determined; dim, forms dimers; tet, forms tetramers; oct, forms octamers. Int, intrinsic operator binding; coop, cooperative operator binding; NS, nonspecific binding to flanking operator DNA up to 50 μM total protein; (parenthesized symbols) represent the relative apparent strength of the process, since there is no true wild-type reference.

DISCUSSION

Ongoing characterization of cooperativity mutants of the λ cI repressor is providing a functional dissection of molecular interactions in this system, revealing selective deficiencies in one or more of the self-association and DNA binding processes in which the protein participates (see Table 6). The present study by analytical ultracentrifugation completes the assembly profiles for wild-type and mutant cI proteins that were initiated using *in vivo* radiolabeled repressors and analytical gel chromatography (Beckett *et al.*, 1993; Burz *et al.*, 1994). The concentration range examined for this family of nearly-identical systems covers a 5-million-fold range, from 10^{-12} to $\sim 5 \times 10^{-5}$ M in total protein and encompasses the processes of dimerization, tetramerization, and octamerization. We have demonstrated that six repressors do not assemble beyond dimers (GD147, EK188, KN192, YH210, SN228, and SR228); two form dimers, probable tetramers and octamers (WT and EK102) (see subsequent discussion); and one exhibits a monomer to octamer process (PT158) with tetramer as a probable intermediate. Our results are in agreement with previous reports of tetramer and octamer formation in this general concentration range (Pirrotta *et al.*, 1970; Chadwick *et al.*, 1973; Brack & Pirrotta, 1975; Banik *et al*., 1993; Senear *et al*., 1993). The possibility of higher order assembly of mutant repressors that remain dimeric up to 50 μM cannot be addressed with the present data; however, concentrations above this range would be far in excess of physiological levels.

The maximal aggregate size and the free energies resolved for wild-type repressor assembly at 20 °C are in excellent agreement with previous data from analytical ultracentrifugation (Senear *et al*., 1993) and are also in good agreement with the equilibrium constant and free energy (2.3×10^{-6} M; −7.7 kcal/mol of tetramer formed) estimated by fluorescence anisotropy for dimer−tetramer association at 25 °C (Banik *et al*., 1993). However, whereas Senear *et al*. endorsed the existence of tetrameric intermediates, they suggested that the resolved energetics predicted that tetramers would never constitute a significant fraction of the population. Banik *et al*. (1993) presented evidence supporting a population of tetramers dominating the ensemble between

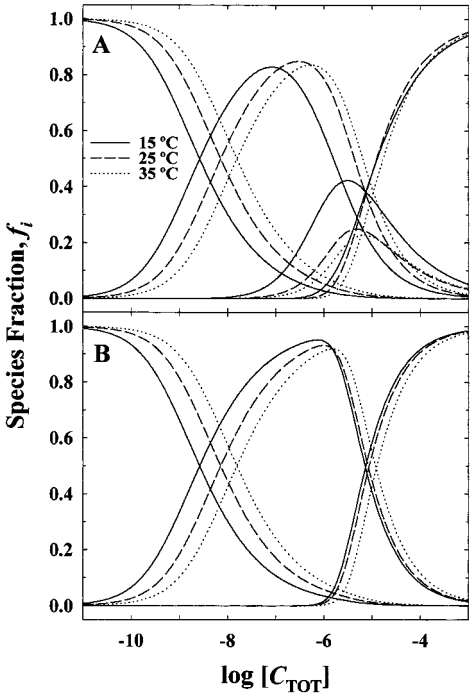

FIGURE 6: Temperature dependence of the mass fraction of each self-associating species of wild-type repressor as a function of total monomer. Assembly free energies used for dimer−octamer, dimer−tetramer, and tetramer−octamer are given in Table 2; the monomer−dimer free energy was −11 kcal/mol. (A) Monomer−dimer−tetramer−octamer assembly model; (B) monomer−dimer−octamer assembly model.

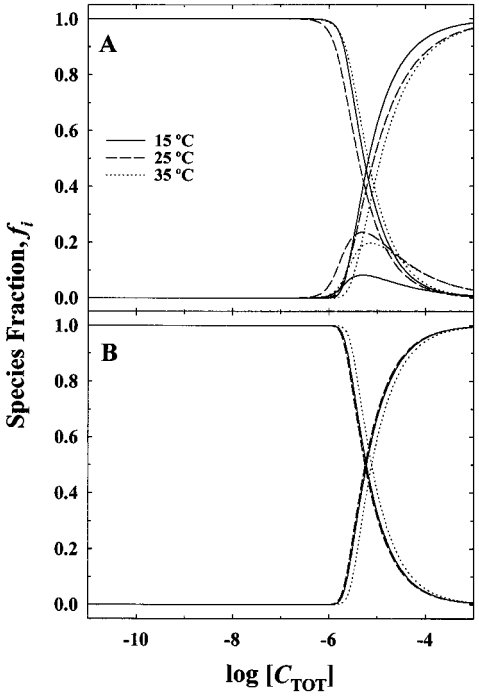

FIGURE 7: Temperature dependence of the mass fraction of each self-associating species of PT158 repressor as a function of total monomer. Assembly free energies used for monomer−octamer, monomer−tetramer, and tetramer−octamer are given in Table 3. (A) Monomer−tetramer−octamer assembly model; (B) monomer−octamer assembly model.

10 and 20 μM. Bandyopadhyay *et al*. (1995) have suggested that the discrepancy between the free energy coupling deduced for the reaction stages of tetramerization and octamerization might be attributed to different solution conditions employed by the two studies.

Our sedimentation data, like that of Senear *et al.* (1983) could not rule out the infinitely cooperative dimer to octamer assembly and provided equally good fits to the dimer−tetramer−octamer model. Given this indeterminancy and the independent evidence for tetrameric species, it would seem inappropriate to dismiss the second stoichiometric model and opt for the infinitely concerted (dimer−octamer) one. Once the decision is made to allow a tetrameric intermediate into the equilibrium scheme of dimer to octamer transition, the relative abundance of tetramers is predicted inexorably by eqs 14−18 from the NONLIN-resolved free energies. This prediction from the results of sedimentation studies (and eqs 14−18) that tetramers have a significant abundance in the assembly pathway is consistent with the original observations of Pirrotta *et al*. (1973) using sedimentation velocity and of Brack and Pirrotta (1975) using sedimentation equilibrium and electron microscopy.

Model-dependent species population distributions for wild-type and PT158 repressors are illustrated, as a function of temperature, in Figures 6 and 7, respectively. The distributions for EK102 are very similar to wild-type. Our analysis of the dimer−tetramer−octamer assembly of wild-type and EK102 repressors at 20 °C indicates that tetramer assembly starts at ∼1 μM total repressor and reaches its largest contribution to the ensemble between 5 and 10 μM. Octamer assembly begins at ∼1 μM and comprises most of the population by 100 μM. The dimer−octamer model predicts a sharper transition (Figure 6). PT158 tetramers begin assembling at 1 μM, and peak between 5 and 15 μM. Assembly to octamers occurs between 1 and 100 μM (Figure 7). The reduction in assembly with increasing temperature shifts the reactions to higher concentrations, in agreement with the temperature dependence of tetramer assembly observed by Banik *et al*. (1993). These authors suggested that tetramers dominate the population between 10 and 20 μM, while the sedimentation data predict that the maximum mass contribution of tetramers would occur at a slightly lower value at 25 °C.

The onset of octamerization is predicted to occur at ∼1 μM monomer concentration whether or not tetrameric intermediates are involved. This threshold applies even for PT158, which is apparently unable to dimerize while free in solution. The free energy of this oligomerization transition is quite large (Tables 2 and 3), suggesting a specific role for either tetramerization and/or octamerization. If tetramers are an intermediate in the assembly pathway for PT158, then the only functional anomaly exhibited by this mutant is the selective loss of dimerization.

Correlation between Oligomerization and Cooperativity. Of the six mutant repressors that self-associate to dimers, five are lacking or defective in cooperative operator DNA binding, the sole exception being SN228 which, although defective in dimerization and unable to oligomerize, binds operator DNA with wild-type cooperativity. Conversely, all three oligomerizing repressors exhibit highly cooperative operator DNA binding (Table 6). These observations suggest that the ability to oligomerize is likely to facilitate but is not required for cooperativity. What then might contribute to the cooperativity observed for SN228? The innate plasticity of repressor monomers upon forming dimers has been shown to be a major determinant in establishing cooperative binding. There may be considerable compaction

of repressor monomers upon dimerization as demonstrated by changes in the hydrated radii of monomeric and dimeric mutant repressors relative to wild type (Burz *et al*., 1994). Mutant monomers that are uniformly larger than wild type assemble to form two size classes of dimers. The smaller of these, typified by EK102 and SN228, have approximately the same Stokes radius as wild type and are highly cooperative. Thus, one may speculate that the structural determinants of the plasticity required to achieve a correct dimer radius and to carry out oligomerization may be related. Furthermore, the DNA itself may play a direct role in cooperative interactions: λ right operator DNA has been shown capable of inducing the formation of DNA-bound dimers from a monomer and octamer pool (Burz & Ackers, 1994; Merabet & Ackers, 1995). Also, residual nonadditivity in the enthalpy and heat capacity changes between the non-cooperative GD147 and wild-type repressors accompanying tripartite right operator binding has led to speculation that structural changes at neighboring sites may result from specific operator site−repressor interactions (Merabet & Ackers, 1995). Finally, induction of bound operator-dependent hypersensitivity in adjacent unoccupied operator sites is alleviated upon occupancy of the adjacent site; the hypersensitive regions map to essentially the same locations within operator sites as those reported by Strahs and Brenowitz (1994) for wild-type repressor (unpublished observations).

Temperature Effects and Enthalpies. Temperature dependence of the assembly energetics was determined for the oligomerizing and weakly dimerizing repressors from 5 to 40 °C; the signs and magnitudes of their thermodynamic contributions to the assembly processes were estimated. These results may be important to approximate the assembly state of cI mutants during *in vivo* experiments aimed at examining the role of cooperativity in the lysogenic to lytic switch and in the maintenance of lysogeny (Shea & Ackers, 1985). Temperature dependence of assembly constants for wild type and EK102 showed overall octamerization to be enthalpically driven in the physiological temperature range and to occur with near-zero heat capacity change (Figure 3, see below). The van't Hoff enthalpies for the assembly of dimers to octamers were estimated to be −14 and −16 kcal/mol for wild type and EK102, respectively; these values are close to the −15 kcal/mol obtained for dimerization of wild-type repressor monomers (Table 5). The wild-type behavior exhibited by EK102 is consistent with its previously determined properties of dimerization and operator DNA binding (Burz *et al*., 1994, Burz & Ackers, 1994). Assembly of PT158 monomers to octamers is accompanied by an enormous apparent enthalpy change between 30 and 40 °C (−101 kcal/mol) and a large negative heat capacity change. Below 30 °C, the van't Hoff enthalpy is estimated at −10 kcal/mol, approximately equal to that for overall assembly of wild-type and EK102 dimers to octamers (Table 5). The drastically different thermal assembly profile of PT158 is probably due to structural consequences resulting from this mutant's selective loss of dimerization. Lastly, the model predictions show the assembly state of PT158 to remain largely temperature invariant until ∼30 °C, whereupon the equilibrium dissociation constant increases from ∼8 to ∼20 μM by 40 °C (Figure 7). In the case of WT and EK102, the assembly state shows a monotonic shift to higher concentrations with increasing temperature (Figure 6).

Assessing the enthalpic and heat capacity changes accompanying stepwise assembly is complicated due to the high correlation between the resolved equilibrium constants K_2 and K_4. Parameter values are strongly biased by subtle variations in the data. While this problem is minimized by collecting data sets over the same range, the temperature-dependent changes in assembly do not ensure that the same range of variation in the mass-average molecular weight will be obtained. While a slight positive slope was suggested by the data for dimer−tetramer assembly, no trends were clear from inspecting the temperature dependence of tetramer−octamer equilibrium constants (Figures 3 and 4). Therefore, enthalpies reported for these processes (Table 5) must be considered approximate. Values estimated for the dimer−tetramer assembly of WT (−9 kcal/mol) and EK102 (−13 kcal/mol) are considerably smaller than the −26 kcal/mol reported by Banik *et al*. (1993). However, the small enthalpy inferred for the tetramer−octamer assembly (Table 5) is consistent with the evidence of very little heat accompanying dilution of octameric WT cI in calorimetric experiments (Merabet & Ackers, 1995).

Dimerization constants obtained for SN228 and SR228 repressors display different temperature dependencies from one another and from wild type (Figure 5). The negative slope for SN228 indicates a van't Hoff enthalpy of +4.6 kcal/mol (Table 5); that for the high temperature limb of SR228 was estimated as −50 kcal/mol, while the low temperature limb yielded +9 kcal/mol. The similarity of low temperature enthalpies suggests that below 25 °C the thermodynamic driving force for dimerization may be the same for these mutants. These enthalpies differ from those of the linear van't Hoff plot of WT dimerization [−15 kcal; Table 5; see also Koblan and Ackers (1991a)]. They demonstrate how disparate thermodynamic profiles for a given process may result from single residue substitutions at a common site and which may underlie the cooperative DNA binding exhibited by these repressors. Wild type and SN228 display full cooperative binding to operator DNA while that of SR228 is reduced by about one half.

Estimates of Heat Capacity Responses. As with the enthalpies, values of ΔC_p accompanying stepwise assembly could not be reliably obtained due to the lack of significant curvature in the van't Hoff plots and the high correlation between resolved ΔC_p and the T_S and T_H (temperatures where ΔS and ΔH equal zero, respectively). By systematically varying the value of ΔC_p and holding it fixed in the fitting process, we were able to approximate the apparent heat capacity change from the minimum and the variation of resulting standard deviations. Unfortunately, the high degree of correlation between T_H and T_S made the fits extremely sensitive to the starting approximations of fitted parameters. Therefore, as with stepwise enthalpies, these values are only rough approximations. The extremely linear van't Hoff plot for the assembly of wild-type and EK102 dimers and for SN228 dimerization indicates a near-zero heat capacity change associated with those processes. A positively sloped linear van't Hoff plot over this temperature range results in a T_H (the temperature at which the enthalpy changes sign) below 0 °C, characteristic of enthalpically driven processes. This signature has been observed for wild-type cI repressor dimerization (Koblan & Ackers, 1991a) and right operator binding (Koblan & Ackers, 1992; Merabet & Ackers, 1995). It is interesting to note that repressors demonstrating a near-

zero ΔC_p accompanying these assembly reactions exhibit fully cooperative DNA binding of dimers. Conversely, nonlinear van't Hoff plots are obtained for the mutant repressors that exhibit reduced dimer cooperativity (SR228) and fail to form dimers (PT158). These variations in apparent heat capacity likely arise from structural changes accompanying the single residue mutations.

Finally, we note that while this work has answered several questions pertaining to the higher order assembly of cI repressor, the biological function associated with this process has yet to be determined (see Table 6). Given that the onset of oligomerization occurs for wild-type repressor at about the same protein concentration that O_R3 is thought to reach saturation, it is reasonable to ask whether site O_R3 ever reaches complete saturation. If not, then does oligomerization provide a means of autogenous control on the expression of cI repressor that does not rely on steric occlusion of RNA polymerase from P_{RM}? Does the formation of oligomeric repressor complexes play a role in autoregulation by acting as either a "storage reservoir" for excess repressor or by providing a dissociating pool to act against inductive events? Or does the formation of higher order repressor species occur outside the concentration range of protein in a lysogenic cell?

ACKNOWLEDGMENT

We thank Andy Herr and Todd Pray for their critical reading and extremely valuable suggestions regarding this study.

REFERENCES

Ackers, G. K., Johnson, A. D., & Shea, M. A. (1982) *Proc. Natl. Acad. Sci. U.S.A. 79*, 1129−1133.
Amann, E., Brosius, J., & Ptashne, M. (1983) *Gene 25*, 167−178.
Bandyopadhyay, S., Banik, U., Bhattacharyya, B., Mandal, N. C., & Roy, S. (1995) *Biochemistry 34*, 5090−5097.
Banik, U., Mandal, N. C., Bhattacharyya, B., & Roy, S. (1993) *J. Biol. Chem. 268*, 3938−3943.
Beckett, D., Koblan, K. S., & Ackers, G. K. (1991) *Anal. Biochem. 196*, 69−75.
Beckett, D., Burz, D. S., Ackers, G. K., & Sauer, R. T. (1993) *Biochemistry 32*, 9073−9079.
Benson, N., Adams, C., & Youderian, P. (1994) *Mol. Microbiol. 11*, 567−579.
Brack, C., & Pirrotta, V. (1975) *J. Mol. Biol. 96*, 139−152.
Brenowitz, M., Senear, D. F., Shea, M. A., & Ackers, G. K. (1986) *Methods Enzymol. 130*, 132−181.
Burz, D. S., & Ackers, G. K. (1994) *Biochemistry 33*, 8406−8416.
Burz, D. S., Beckett, D., Benson, N., & Ackers, G. K. (1994) *Biochemistry 33*, 8399−8405.
Chadwick, P., Pirrotta, V., Steinberg, R., Hopkins, N., & Ptashne, M. (1973) *Cold Spring Harbor Symp. Quant. Biol. 35*, 283−294.
Gimble, F. S., & Sauer, R. T. (1989) *J. Mol. Biol. 206*, 29−39.
Johnson, A. D. (1980) Ph.D. Thesis, Harvard University, Cambridge, MA.
Johnson, A. D., Poteete, A. R., Lauer, G., Sauer, R. T., Ackers, G. K., & Ptashne, M. (1981) *Nature 294*, 217−223.
Johnson, M. L., Correia, J. J., Yphantis, D. A., & Halvorson, H. R. (1981) *Biophys. J. 36*, 575−588.
Koblan, K. S., & Ackers, G. K. (1991a) *Biochemistry 30*, 7817−7821.
Koblan, K. S., & Ackers, G. K. (1991b) *Biochemistry 30*, 7822−7827.
Koblan, K. S., & Ackers, G. K. (1992) *Biochemistry 31*, 57−65.
Laemmli, U. (1970) *Nature 227*, 680−685.
Laue, T. M., Johnson, A. E., Esmon, C. T., & Yphantis, D. A. (1984) *Biochemistry 23*, 1339−1348.
Laue, T. M., Shah, B. D., Ridgeway, T. M., & Pelletier, S. L. (1992) in *Analytical Ultracentrifugation in Biochemistry and Polymer Science* (Harding, S., Rowe, A., & Horton, J. C., Eds.) pp 90−125, Royal Society of Chemistry, London.
Merabet, E., & Ackers, G. K. (1995) *Biochemistry 34*, 8554−8563.
Pabo, C. O., Sauer, R. T., Sturtevant, J. M., & Ptashne, M. (1979) *Proc. Natl. Acad. Sci. U.S.A. 76*, 1608−1612.
Pirrotta, V., Chadwick, P., & Ptashne, M. (1970) *Nature 227*, 41−44.
Ptashne, M. (1992) *A Genetic Switch*, 2nd ed., Cell Press and Blackwell Scientific Publications, Cambridge, MA.
Sauer, R. T., & Anderegg, R. (1978) *Biochemistry 17*, 1092−1100.
Senear, D. F., & Ackers, G. K. (1990) *Biochemistry 29*, 6568−6577.
Senear, D. F., & Batey, R. (1991) *Biochemistry 30*, 6677−88.
Senear, D. F., Laue T. M., Ross, J. B. A., & Waxman, E. (1993) *Biochemistry 32*, 6179−6189.
Shea, M. A., & Ackers, G. K. (1985) *J. Mol. Biol. 181*, 211−230.
Strahs, D., & Brenowitz, M. (1994) *J. Mol. Biol. 24*, 494−510.

BI952055X